

Article

Stability of Cs/Ru/MgO Catalyst for Ammonia Synthesis as a Hydrogen and Energy Carrier

Rahat Javaid ^{*}  and Tetsuya Nanba

Renewable Energy Research Center, Fukushima Renewable Energy Institute, National Institute of Advanced Industrial Science and Technology (AIST), 2-2-9 Machiikedai, Koriyama 963-0298, Fukushima, Japan; tty-namba@aist.go.jp

* Correspondence: rahat.javaid@aist.go.jp; Tel.: +81-29-861-3412

Abstract: The Cs/Ru/MgO catalyst was synthesized by sequential impregnation of Ru and Cs on MgO support using Ru(NO₃)₃ and CsNO₃ precursors. Catalytic ammonia synthesis was carried out in a fixed-bed flow reactor using H₂ and N₂ as reactants. The stability of the catalyst was measured at 350 °C, 2.5 MPa gauge pressure, and SV as 1200 h⁻¹ using the H₂/N₂ ratio 3 as a reactant feedstock. The Cs/Ru/MgO catalyst retained its ammonia synthesis activity while conducting experiments at mild reaction conditions of 325 °C and 350 °C. An increase in experimental temperature to 375–425 °C decreased the ammonia synthesis activity retaining only to 42% of the initial activity after 680 h of time on stream. The deformation of the catalyst's structure, which was caused by Cs leaching and redistribution of the Ru and increased crystallinity of MgO at high-temperature conditions, was considered the plausible reason for the drastic decrease in ammonia synthesis activity.

Keywords: ammonia synthesis; catalyst stability; Cs promoter; MgO support; Ru catalyst



Citation: Javaid, R.; Nanba, T. Stability of Cs/Ru/MgO Catalyst for Ammonia Synthesis as a Hydrogen and Energy Carrier. *Energies* **2022**, *15*, 3506. <https://doi.org/10.3390/en15103506>

Academic Editor: Mohan Lal Kolhe

Received: 12 April 2022

Accepted: 10 May 2022

Published: 11 May 2022

Publisher's Note: MDPI stays neutral with regard to jurisdictional claims in published maps and institutional affiliations.



Copyright: © 2022 by the authors. Licensee MDPI, Basel, Switzerland. This article is an open access article distributed under the terms and conditions of the Creative Commons Attribution (CC BY) license (<https://creativecommons.org/licenses/by/4.0/>).

1. Introduction

Ammonia production was considerably increased worldwide during the twentieth century, and nowadays ammonia is among the most produced chemicals [1,2]. Ammonia is an important feedstock to produce fertilizers and has the potential as a hydrogen and energy carrier because of its high hydrogen capacity (17.6 wt-%) and energy density (12.8 GJ m⁻³). Ammonia has a well-established infrastructure for storage and worldwide distribution [3,4]. As combustion of ammonia does not release carbon dioxide (CO₂), it is considered a CO₂-free fuel with a much higher energy density than compressed hydrogen and closer to fossil fuels [5,6]. Ammonia is industrially synthesized by the Haber–Bosch process requiring high temperature (425–600 °C) and pressure (20–30 MPa) conditions, which account for 1–2% of global energy consumption [7,8]. Most of the energy consumed by the ammonia plant is utilized in hydrogen production from natural gas and its conversion to ammonia. Globally, the Haber–Bosch process employs around 5% of natural gas causing a worldwide CO₂ emission of 1.5%. Therefore, overall, ammonia synthesis is known to be an energy and capital-intensive and environmentally unfriendly chemical process. To reduce energy consumption and CO₂ emissions, it is suggested to produce CO₂-free ammonia at a plant scale utilizing renewable-derived hydrogen at mild temperature and pressure conditions. Ruthenium (Ru)-based catalysts have been recognized for their capability to produce ammonia at milder reaction conditions than required by the iron-based catalyst used in the Haber–Bosch process [9–12]. Generally, cleavage of the high-energy N–N triple bond (945 kJ mol⁻¹) of nitrogen is considered as the rate-determining step for ammonia synthesis. The most effective way to accelerate this rate-determining step is to enhance the electron density of Ru particles by use of basic support or promoter [13,14]. The material used as support greatly influences the efficiency of the catalyst. Industrially, graphitized carbon has been used as support for Ru in the Kellogg Brown and Root Advanced Ammonia Process (KBRAAP) [15,16], but the methanation of the carbon support causes degradation of the

catalyst [17,18]. Various noncarbon materials, such as Al_2O_3 [19], MgO [20], MgAl_2O_4 [21], zeolites [10], etc., were evaluated for their activities for ammonia synthesis. Among various supports, MgO was proposed as a stable and active support for Ru catalysts capable of higher efficiency at a relatively lower temperature of 300–425 °C [22]. In addition to the effect of support materials, alkali and alkaline earth metals are suggested to promote ammonia synthesis when coupled with Ru [20,22]. These promoters improve the electron density as well as dispersion of Ru particles [23–26]. An intensive increase in ammonia synthesis activity was reported for the MgO -supported Ru catalyst on the addition of the promoter in an order of $\text{Cs}^+ > \text{Rb}^+ > \text{K}^+ > \text{Na}^+$ [27]. The ammonia synthesis efficiency of the Ru catalysts is suggested to be strongly dependent on the basicity and electronegativity of the support and promoter [27,28]. The mechanism involves the transfer of electrons from support and promoters to the Ru [23,29] from where these electrons are transferred to the antibonding orbitals of adsorbed nitrogen molecules weakening their N–N triple bonds thereby promoting the dissociation of dinitrogen. The addition of Cs as a promoter to the MgO -supported Ru catalyst is considered for enhancing the ammonia synthesis activity of the catalyst [27,30]. A combination of Cs, Ru, and MgO has been used as a benchmark in many studies.

Considering the potential applications of ammonia, the development of efficient catalysts has been widely investigated at the laboratory scale. However, the scenario for plant-scale application is quite different than for laboratory-scale. The laboratory-scale evaluation at a limited set of reaction conditions and short time stability is not sufficient to evaluate the fate of the catalyst when applied to plant-scale applications, especially when renewable-derived hydrogen is considered as a feedstock. As renewable-derived hydrogen exhibits fluctuating behavior, it is challenging to maintain a fixed reaction condition for the plant-scale operation. For the plant-scale ammonia synthesis application of the catalyst, it is highly desired to conduct a comprehensive study on the effect of reaction conditions on the activity and long-term stability of the catalyst. Cs/Ru/MgO is a well-recognized catalyst for its exceptional ammonia synthesis activity. In our previous published paper [20], a detailed investigation was conducted to evaluate the effects of reaction conditions including the temperature, pressure, and H_2/N_2 ratio on the ammonia synthesis activity of the Cs/Ru/MgO catalyst to establish the available optimum range of reaction conditions. The present study is a continuation of our previous work on the Cs/Ru/MgO catalyst. In this paper, we investigated the trend of stability of the Cs/Ru/MgO catalyst for long-term ammonia synthesis activity. This study is of great importance for the development of a catalyst for the long-term activity to produce ammonia at a plant scale as a carrier of renewable-derived hydrogen and energy.

2. Experimental

2.1. Preparation of Catalyst

MgO was purchased from Merck and used as support. At first, MgO was calcined at 500 °C for 2 h under airflow. A total of 2 wt-% Ru was loaded on MgO support by the impregnation method using $\text{Ru}(\text{NO}_3)_3$ precursor. For this purpose, the calculated amount of MgO was added to the aqueous solution of $\text{Ru}(\text{NO}_3)_3$ and then dried at 100 °C for 18 h in the oven. The dried Ru-loaded MgO catalyst was crushed well to make powder and then reduced to 300 °C for 2 h under a flow of 10% H_2 and 90% N_2 mixture. The resultant powder was assigned as Ru/MgO (Ru-loaded MgO), which was loaded with 6.8 wt-% Cs by the impregnation method using CsNO_3 precursor, followed by drying at 100 °C for 18 h. The catalyst was reduced again to the same conditions of 300 °C for 2 h under a flow of 10% H_2 and 90% N_2 mixture and was denoted as the Cs/Ru/MgO catalyst. The catalyst was sieved to a particle size of 60–100 mesh.

2.2. Characterization

The HAADF-STEM and EDS analysis were conducted to determine the morphology of the as-synthesized and used (after 680 h of time on stream) catalysts. The XRD patterns

were measured by RINT-Ultima, RIGAKU, Tokyo, Japan in the range of $2\theta = 20^\circ - 80^\circ$ at a speed of $2^\circ/\text{min}$ with 0.01° steps. Nitrogen adsorption was measured by BELSORP-mini II, (MicrotracBEL Corp., Osaka, Japan), and then the specific surface area was estimated by the Brunauer–Emmett–Teller (BET) method. The loadings of deposited Ru and Cs were analyzed by inductively coupled plasma-optical emission spectroscopy (ICP-OES) (7500i; Agilent, Santa Clara, CA, USA).

2.3. Catalytic Activity for Ammonia Synthesis

The evaluation of the Cs/Ru/MgO catalyst for ammonia synthesis activity and stability was conducted in a fixed-bed reactor. Prior to ammonia synthesis experiments, the catalyst was activated in a flowing gas mixture of 75% H_2 and 25% N_2 at 600°C and ambient pressure for 30 min. The stability experiments were conducted at the standard condition of 350°C , 2.5 MPa gauge pressure, H_2/N_2 ratio 3, and SV as 1200 h^{-1} using H_2 and N_2 gases as reactants. The concentration of ammonia produced was measured by passing the outlet gases from the aqueous solution of sulfuric acid (H_2SO_4) [7,20,31–33] with an immersed conductivity cell. The rate of ammonia formation was calculated by detecting the decrease in the conductivity of the H_2SO_4 solution (0.4 wt-%) with respect to time. The rate of ammonia synthesis is described in terms of the space–time yield (STY).

3. Results and Discussions

As described earlier, this study is a continuation of our previous research on the Cs/Ru/MgO catalyst. The effects of various reaction conditions including the H_2/N_2 ratio in reactant stream, experimental temperature, gauge pressure, and space velocity were analyzed and explained in our previously published paper [20]. This paper describes the stability trend of the catalyst during a time on stream of 680 h. The activity tests were conducted in five sequences to elucidate the effect of the H_2/N_2 ratio and gauge pressure firstly at the lowest temperature condition of 325°C and then at 350, 375, 400, and 425°C , respectively (Please refer to Figure S1 of the Supplementary Materials). The stability tests were conducted intermittently during the above-mentioned activity mapping against various reaction conditions. Figure 1 demonstrates the stability of the catalyst with time on stream.

According to the results of these durability tests, the catalytic activity was almost constant for 150 h of time on stream with the STY value of $2.1\text{ mmol-NH}_3/\text{g-cat/h}$. These initial 150 h of time on stream represent a period for the activity tests under the lowest experimental temperature condition of 325°C , whereas with an increase in the temperature for the activity experiments to 350, 375, 400, and 425°C , the durability tests showed a rapid decline in catalytic activity, retaining 42% of the initial activity (STY value as $0.86\text{ mmol-NH}_3/\text{g-cat/h}$) after 680 h of time on stream. High-temperature experimental conditions could be a possible factor retarding the activity of the Cs/Ru/MgO catalyst.

To understand the possibilities of deactivation in detail, the as-synthesized catalyst and the catalyst after 680 h of time on stream (used catalyst) were characterized by BET, XRD, TEM, and ICP measurements and compared for changes. The surface area of the as-prepared catalyst was $40\text{ m}^2/\text{g}$, which decreased to less than half ($19\text{ m}^2/\text{g}$) for the used catalyst. Figure 2 illustrates the nitrogen adsorption–desorption isotherms (BET measurement curves) and pore size distribution of the as-synthesized (Figure 2a) and used (Figure 2b) Cs/Ru/MgO catalysts, respectively. According to Figure 2, the nitrogen adsorption–desorption isotherm changed from type IV for the as-synthesized catalyst to type III for the used catalyst. The pore size distributions are demonstrated in the inset images in Figure 2a,b, respectively, which were calculated from their desorption data with the Barret–Joyner–Halenda (BJH) model. The pore size distributions were quite different for the catalyst before and after 680 h of time on stream. For the as-synthesized catalyst, most of the pores were within a diameter of 10 nm, whereas for the used catalyst, large parts of the pores ranged above 10 nm. Thus, the surface area and pore size distribution varied to a large extent for the Cs/Ru/MgO catalyst before and after a time on stream of

680 h, which indicates a diverse change in the texture of the catalyst after a time on stream of 680 h.

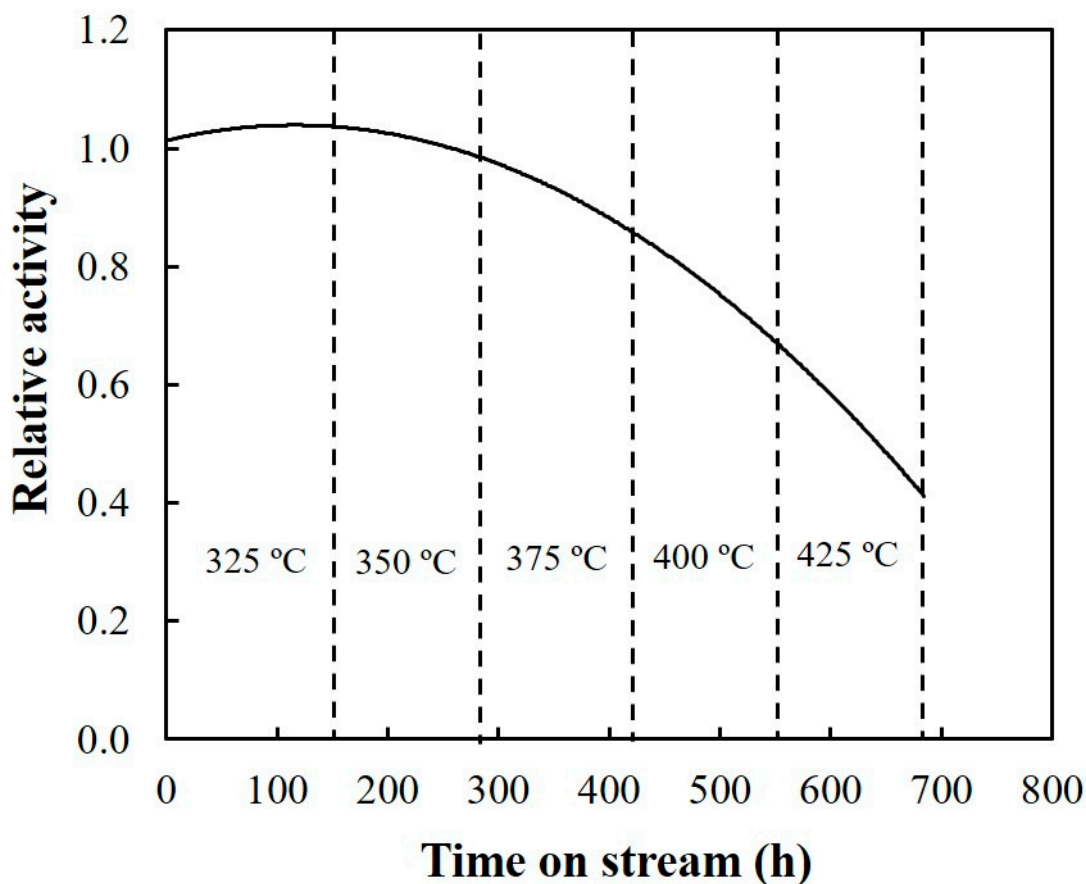


Figure 1. Stability trend of the catalyst with time on stream at different temperature conditions.

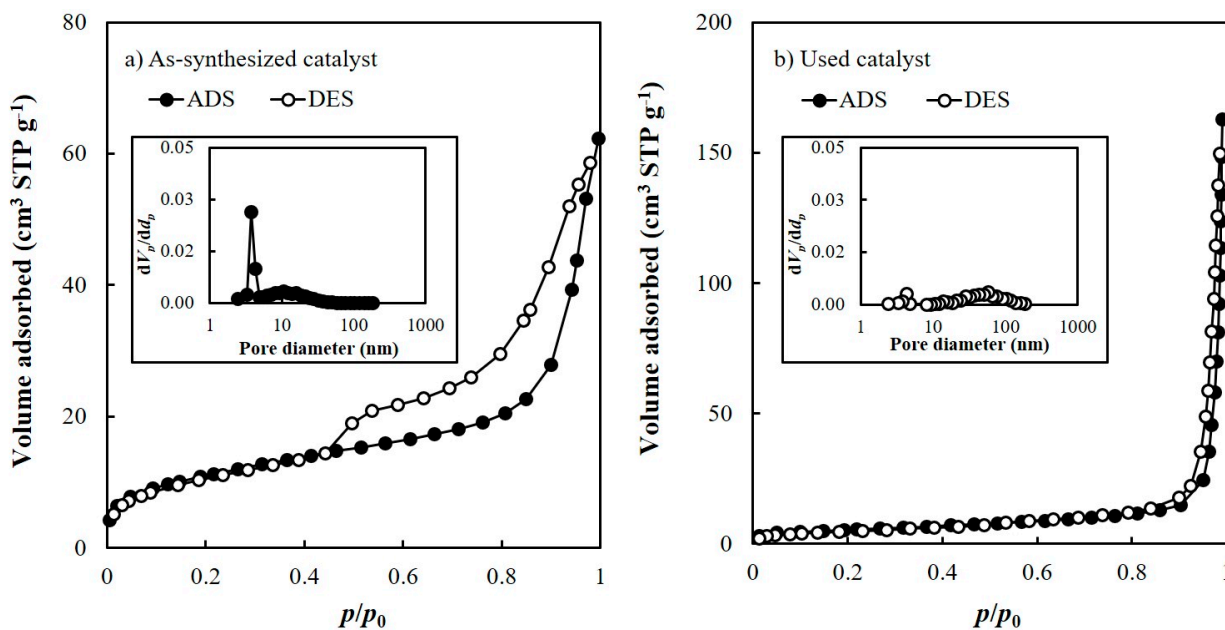


Figure 2. Nitrogen adsorption–desorption isotherms. The insets in figures present the pore size distribution among as-synthesized and used Cs/Ru/MgO catalysts.

Figure 3 presents the XRD patterns for the as-synthesized and used Cs/Ru/MgO catalysts. According to the XRD pattern of the as-synthesized catalyst (Figure 3a), the diffraction peaks at $2\theta = 38.0^\circ$, 51.0° , and 58.8° were assigned to $\text{Mg}(\text{OH})_2$. Peaks for MgO appeared at $2\theta = 42.7^\circ$ and 61.8° [20,34]. No peak for the Ru or Cs species was noticed, which indicates that these particles are amorphous or smaller in diameter than the detection limit of the diffractometer, whereas highly intense diffraction peaks appeared for the used catalyst (Figure 3b), indicating the highly ordered crystalline structure of MgO. Hence, the results from nitrogen adsorption and XRD analysis suggest changes in the morphology of the catalyst with time on stream.

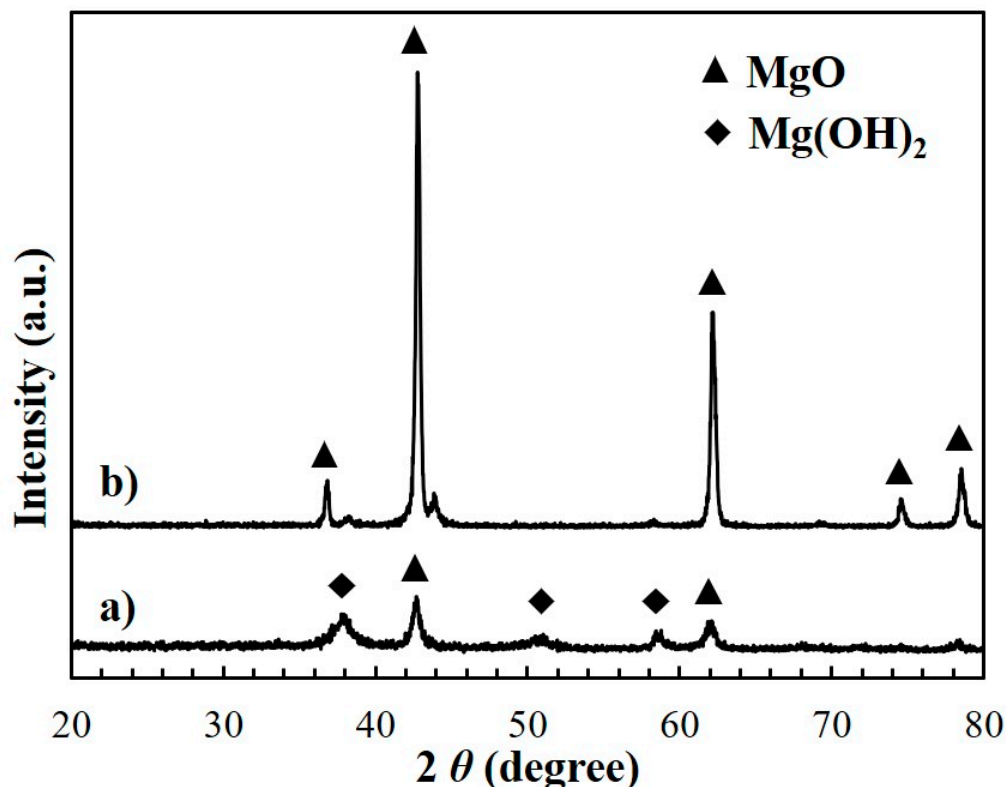


Figure 3. XRD pattern of Cs/Ru/MgO catalyst: (a) as-synthesized catalyst and (b) used catalyst after reaction of 680 h.

To confirm the morphological and structural changes of the catalyst, a HAADF-STEM analysis coupled with EDS was conducted (Figure 4). The elemental mapping of as-synthesized catalyst (Figure 4a) showed the high dispersion of Ru and Cs on MgO support, whereas comparatively larger Ru particles and a highly crystalline structure of MgO support were observed for the used catalyst (Figure 4b). The histogram (Figure 4c) illustrates the distribution of Ru particle size on MgO support after 680 h of time on stream (used catalyst). A total of 150 Ru particles were counted, with an average particle size within a range of 4–10 nm, which confirms the agglomeration of the Ru particles. STEM images also revealed a substantial decrease in the Cs content in the used catalyst.

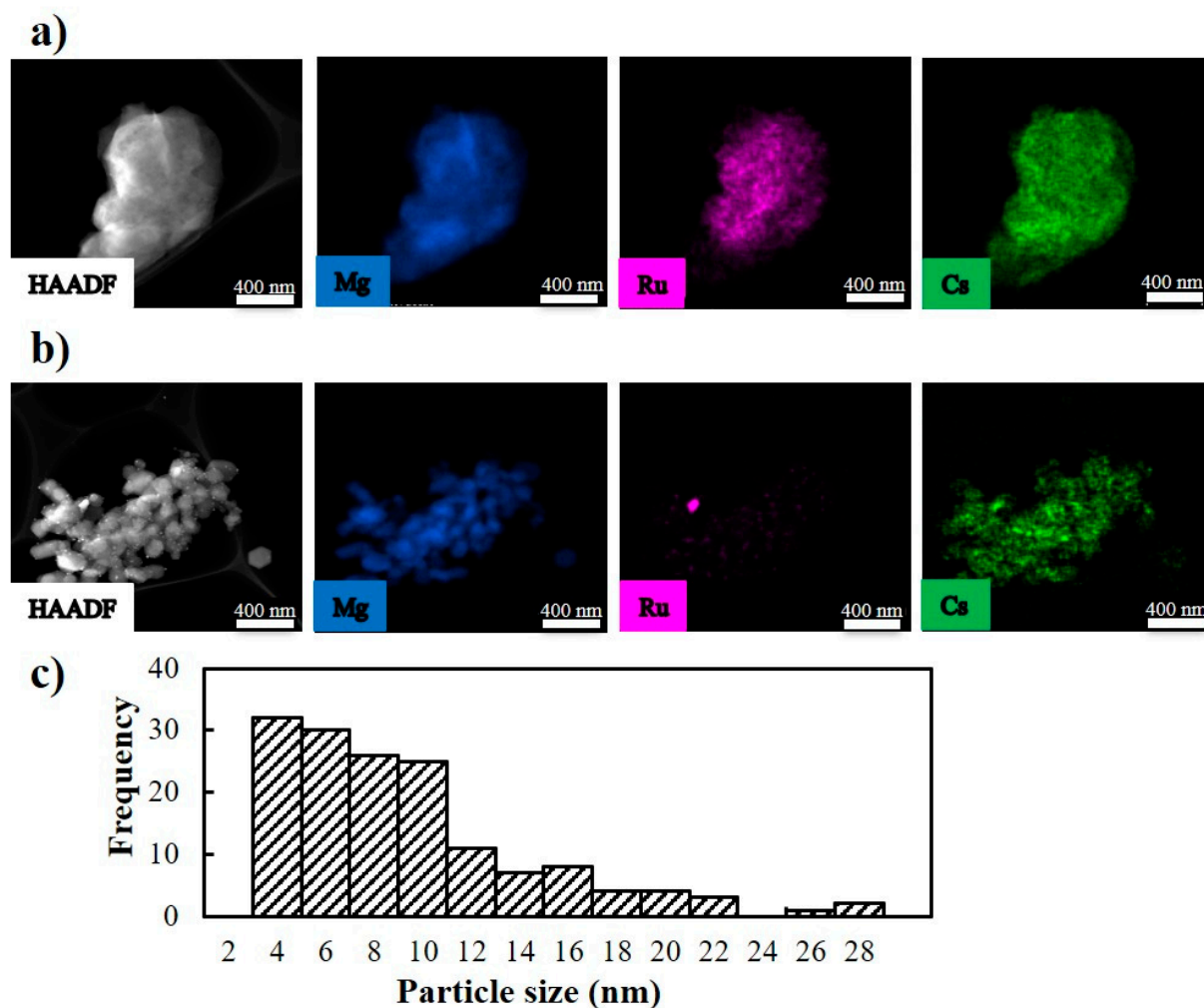


Figure 4. HAADF-STEM images with elemental mapping for Mg, Ru, and Cs: (a) as-synthesized catalyst, (b) after a time on stream of 680 h, and (c) histogram of the particle size distribution of Ru in the used catalyst after 680 h of time on stream.

The leaching of Cs was confirmed by ICP analysis. The Cs content decreased from 6.4 wt-% in the as-synthesized catalyst to 0.8 wt-% in the used catalyst after a time on stream of 680 h. As cesium oxide was loaded on the surface of the catalyst, leaching dramatically decreased the surface concentration of Cs, which led to the drastic decrease in catalytic activity. Larichev et al. [35] studied the chemical state of the Cs promoter and revealed the presence of a mixture of cesium oxide (Cs_2O) and cesium peroxide (Cs_2O_2) in the Cs/Ru/MgO catalyst. The authors of [35] also suggested that close contact between the Cs promoter and Ru particles resulted in sufficiently high catalytic activity for ammonia synthesis by introducing a high dispersion of Ru on the surface of the catalyst and also by enhancing the electron density caused by the donation of electrons from cesium oxide to Ru. Rosowski et al. [36] confirmed that the Cs species have less affinity for basic supports such as MgO. In the present study, the high dispersion of the Ru particles was confirmed in the as-prepared Cs/Ru/MgO catalyst in the presence of Cs. However, the Cs species have very low melting points of 297.8 °C and 490 °C for Cs_2O and Cs_2O_2 , respectively. Therefore, a low melting point and less affinity of the Cs species with MgO support decreased the stability of the Cs species ultimately causing the leaching and dislocation of the Cs species during ammonia synthesis experiments at high-temperature conditions. As a consequence, it is suggested that the high-temperature operation caused structural and morphological changes in the Cs/Ru/MgO catalyst including leaching of the Cs promoter, reconstruction, and rearrangement of MgO support toward the more organized crystalline

structure with a lower surface area and agglomeration of Ru metal, which reduced the active sites of the catalyst. These structural changes associated with the high temperature retarded the catalytic activity of Cs/Ru/MgO for ammonia synthesis. Therefore, it is of pivotal importance to evaluate a catalyst for long-term stability especially if a large-scale application is desired.

4. Conclusions

In conclusion, the Cs/Ru/MgO catalyst was prepared by the impregnation method and evaluated for the activity and stability for ammonia synthesis. The stability of the catalyst was observed within a time on stream of 680 h. The operation at a relatively high temperature of 350–425 °C greatly changed the composition, structure, and morphology of the Cs/Ru/MgO catalyst. The crystallization of MgO, leaching of Cs, and redistribution and agglomeration of Ru occurred at higher operating temperature conditions. The structural changes along with the leaching of the Cs promoter retarded the catalytic activity of Cs/Ru/MgO for ammonia synthesis. Such a study for the evaluation of the long-term stability of the catalyst is essential to achieve the plant-scale ammonia synthesis application.

Supplementary Materials: The following supporting information can be downloaded at: <https://www.mdpi.com/article/10.3390/en15103506/s1>, Figure S1: Effect of reaction conditions on space-time yield (STY) of Cs/Ru/MgO catalyst for ammonia synthesis.

Author Contributions: Conceptualization, R.J. and T.N.; methodology, R.J. and T.N.; validation R.J. and T.N.; formal analysis, R.J.; investigation, R.J.; writing—original draft preparation, R.J.; writing—review and editing, R.J. and T.N.; visualization, R.J. and T.N. All authors have read and agreed to the published version of the manuscript.

Funding: This research received no external funding.

Institutional Review Board Statement: Not applicable.

Informed Consent Statement: Not applicable.

Data Availability Statement: Not applicable.

Conflicts of Interest: The authors declare no conflict of interest.

References

1. Lan, R.; Irvine, J.T.S.; Tao, S. Ammonia and Related Chemicals as Potential Indirect Hydrogen Storage Materials. *Int. J. Hydrog. Energy* **2012**, *37*, 1482–1494. [CrossRef]
2. Makepeace, J.W.; Wood, T.J.; Hunter, H.M.A.; Jones, M.O.; David, W.I.F. Ammonia Decomposition Catalysis Using Non-Stoichiometric Lithium Imide. *Chem. Sci.* **2015**, *6*, 3805–3815. [CrossRef] [PubMed]
3. Miura, D.; Tezuka, T. A Comparative Study of Ammonia Energy Systems as a Future Energy Carrier, with Particular Reference to Vehicle Use in Japan. *Energy* **2014**, *68*, 428–436. [CrossRef]
4. Zamfirescu, C.; Dincer, I. Using Ammonia as a Sustainable Fuel. *J. Power Sources* **2008**, *185*, 459–465. [CrossRef]
5. Dimitriou, P.; Javaid, R. A Review of Ammonia as a Compression Ignition Engine Fuel. *Int. J. Hydrog. Energy* **2020**, *45*, 7098–7118. [CrossRef]
6. Javaid, R. Catalytic Hydrogen Production, Storage and Application. *Catalysts* **2021**, *11*, 836. [CrossRef]
7. Javaid, R.; Nanba, T. Effect of Preparation Method and Reaction Parameters on Catalytic Activity for Ammonia Synthesis. *Int. J. Hydrog. Energy* **2021**, *46*, 35209–35218. [CrossRef]
8. Kuang, A.; Zhou, T.; Wang, G.; Li, Y.; Wu, G.; Yuan, H.; Chen, H.; Yang, X. Dehydrogenation of Ammonia Borane Catalyzed by Pristine and Defective H-BN Sheets. *Appl. Surf. Sci.* **2016**, *362*, 562–571. [CrossRef]
9. Forni, L.; Molinari, D.; Rossetti, I.; Pernicone, N. Carbon-Supported Promoted Ru Catalyst for Ammonia Synthesis. *Appl. Catal. A Gen.* **1999**, *185*, 269–275. [CrossRef]
10. McClaine, B.C.; Davis, R.J. Importance of Product Readsorption during Isotopic Transient Analysis of Ammonia Synthesis on Ba-Promoted Ru/BaX Catalyst. *J. Catal.* **2002**, *211*, 379–386. [CrossRef]
11. Izumi, Y.; Iwata, Y.; Aika, K. Catalysis on Ruthenium Clusters Supported on CeO₂ or Ni-Doped CeO₂: Adsorption Behavior of H₂ and Ammonia Synthesis. *Society* **1996**, *2*, 9421–9428. [CrossRef]
12. Javaid, R.; Nanba, T. Effect of Texture and Physical Properties of Catalysts on Ammonia Synthesis. *Catal. Today* **2021**, *in press*. [CrossRef]

13. Javaid, R.; Nanba, T. MgFe₂O₄-Supported Ru Catalyst for Ammonia Synthesis: Promotive Effect of Chlorine. *ChemistrySelect* **2020**, *5*, 4312–4315. [[CrossRef](#)]
14. Javaid, R.; Aoki, Y.; Nanba, T. Highly Efficient Ru/MgO–Er₂O₃ Catalysts for Ammonia Synthesis. *J. Phys. Chem. Solids* **2020**, *146*, 109570. [[CrossRef](#)]
15. You, Z.; Inazu, K.; Aika, K.; Baba, T. Electronic and Structural Promotion of Barium Hexaaluminate as a Ruthenium Catalyst Support for Ammonia Synthesis. *J. Catal.* **2007**, *251*, 321–331. [[CrossRef](#)]
16. Truskiewicz, E.; Raróg-Pilecka, W.; Schmidt-Szałowski, K.; Jodzis, S.; Wilczkowska, E.; Łomot, D.; Kaszukur, Z.; Karpiński, Z.; Kowalczyk, Z. Barium-Promoted Ru/Carbon Catalyst for Ammonia Synthesis: State of the System When Operating. *J. Catal.* **2009**, *265*, 181–190. [[CrossRef](#)]
17. Nanba, T.; Javaid, R.; Matsumoto, H. Ammonia Synthesis Catalyst Development for Renewable Energy Storage. *Fine Chem.* **2019**, *48*, 6–11.
18. Nanba, T.; Javaid, R.; Matsumoto, H. Ammonia Synthesis by Using Hydrogen Produced from Renewable Energy. *Catalysts Catal.* **2019**, *61*, 66–71.
19. Lin, B.; Wang, R.; Lin, J.; Du, S.; Yu, X.; Wei, K. Preparation of Chlorine-Free Alumina-Supported Ruthenium Catalyst for Ammonia Synthesis Base on RuCl₃ by Hydrazine Reduction. *Catal. Commun.* **2007**, *8*, 1838–1842. [[CrossRef](#)]
20. Javaid, R.; Matsumoto, H.; Nanba, T. Influence of Reaction Conditions and Promoting Role of Ammonia Produced at Higher Temperature Conditions in Its Synthesis Process over Cs-Ru/MgO Catalyst. *ChemistrySelect* **2019**, *4*, 2218–2224. [[CrossRef](#)]
21. Jacobsen, C.J.H.; Dahl, S.; Hansen, P.L.; Törnqvist, E.; Jensen, L.; Topsøe, H.; Prip, D.V.; Møenshaug, P.B.; Chorkendorff, I. Structure Sensitivity of Supported Ruthenium Catalysts for Ammonia Synthesis. *J. Mol. Catal. A Chem.* **2000**, *163*, 19–26. [[CrossRef](#)]
22. Aika, K.; Takano, T.; Murata, S. Preparation and Characterization of Chlorine-Free Ruthenium Catalysts and the Promoter Effect in Ammonia Synthesis. 3. A Magnesia-Supported Ruthenium Catalyst. *J. Catal.* **1992**, *136*, 126–140. [[CrossRef](#)]
23. Larichev, Y.V.; Moroz, B.L.; Moroz, E.M.; Zaikovskii, V.I.; Yunusov, S.M.; Kalyuzhnaya, E.S.; Shur, V.B.; Bukhtiyarov, V.I. Effect of the Support on the Nature of Metal-Promoter Interactions in Ru-Cs⁺/MgO and Ru-Cs⁺-Al₂O₃ catalysts for Ammonia Synthesis. *Kinet. Catal.* **2005**, *46*, 891–899. [[CrossRef](#)]
24. Kowalczyk, Z.; Krukowski, M.; Raróg-Pilecka, W.; Szmigiel, D.; Zielinski, J. Carbon-Based Ruthenium Catalyst for Ammonia Synthesis: Role of the Barium and Caesium Promoters and Carbon Support. *Appl. Catal. A Gen.* **2003**, *248*, 67–73. [[CrossRef](#)]
25. Zheng, X.; Zhang, S.; Xu, J.; Wei, K. Effect of Thermal and Oxidative Treatments of Activated Carbon on Its Surface Structure and Suitability as a Support for Barium-Promoted Ruthenium in Ammonia Synthesis Catalysts. *Carbon N. Y.* **2002**, *40*, 2597–2603. [[CrossRef](#)]
26. Rossetti, I.; Pernicone, N.; Forni, L. Promoters Effect in Ru/C Ammonia Synthesis Catalyst. *Appl. Catal. A Gen.* **2001**, *208*, 271–278. [[CrossRef](#)]
27. Larichev, Y.V.; Moroz, B.L.; Zaikovskii, V.I.; Yunusov, S.M.; Kalyuzhnaya, E.S.; Shur, V.B.; Bukhtiyarov, V.I. XPS and TEM Studies on the Role of the Support and Alkali Promoter in Ru/MgO and Ru-Cs+ZMgO Catalysts for Ammonia-Synthesis. *J. Phys. Chem. C* **2007**, *111*, 9427–9436. [[CrossRef](#)]
28. Hikita, T.; Aika, K. Alkali Nitrate Promoted Raney Ru Catalyst as a Superior Catalyst for Ammonia Synthesis. *Catal. Lett.* **1990**, *4*, 157–161. [[CrossRef](#)]
29. Aika, K.; Kubota, J.; Kadowaki, Y.; Niwa, Y.; Izumi, Y. Molecular Sensing Techniques for the Characterization and Design of New Ammonia Catalysts. *Appl. Surf. Sci.* **1997**, *121*, 488–491. [[CrossRef](#)]
30. Aika, K.; Ohya, A.; Ozaki, A.; Inoue, Y.; Yasumori, I. Support and Promoter Effect of Ruthenium Catalyst. II. Ruthenium/Alkaline Earth Catalyst for Activation of Dinitrogen. *J. Catal.* **1985**, *92*, 305–311. [[CrossRef](#)]
31. Nanba, T.; Nagata, Y.; Kobayashi, K.; Javaid, R.; Atsumi, R.; Nishi, M.; Mochizuki, T.; Manaka, Y.; Kojima, H.; Tsujimura, T.; et al. Explorative Study of a Ru/CeO₂ Catalyst for NH₃ Synthesis from Renewable Hydrogen and Demonstration of NH₃ Synthesis under a Range of Reaction Conditions. *J. Jpn. Pet. Inst.* **2021**, *64*, 1–9. [[CrossRef](#)]
32. Queiroz, A.; Pedroso, G.B.; Kuriyama, S.N.; Fidalgo-Neto, A.A. Subcritical and Supercritical Water for Chemical Recycling of Plastic Waste. *Curr. Opin. Green Sustain. Chem.* **2020**, *25*, 100364. [[CrossRef](#)]
33. Javaid, R.; Nanba, T. Effect of Reaction Conditions and Surface Characteristics of Ru/CeO₂ on Catalytic Performance for Ammonia Synthesis as a Clean Fuel. *Int. J. Hydrog. Energy* **2021**, *46*, 18107–18115. [[CrossRef](#)]
34. Javaid, R.; Nanba, T. Optimization of reaction conditions for ammonia synthesis using Ru/Cs/MgO catalyst. In Proceedings of the WHEC 2016—21st World Hydrogen Energy Conference 2016, Zaragoza, Spain, 13–16 June 2016.
35. Larichev, Y.V.; Moroz, B.L.; Bukhtiyarov, V.I. Electronic State of Ruthenium Deposited onto Oxide Supports: An XPS Study Taking into Account the Final State Effects. *Appl. Surf. Sci.* **2011**, *258*, 1541–1550. [[CrossRef](#)]
36. Rosowski, F.; Hornung, A.; Hinrichsen, O.; Herein, D.; Muhler, M.; Ertl, G. Ruthenium catalysts for ammonia synthesis at high pressures: Preparation, characterization, and power-law kinetics. *Appl. Catal. A Gen.* **1997**, *151*, 443–460. [[CrossRef](#)]